Lifetimes of optical phonons in graphene and graphite by time-resolved incoherent anti-Stokes Raman scattering

Kwangu Kang,* Daner Abdula, David G. Cahill, and Moonsub Shim
Frederick Seitz Materials Research Laboratory, and Department of Materials Science and Engineering, University of Illinois, Urbana, Illinois 61801, USA
(Received 4 March 2010; published 2 April 2010)

We report lifetimes of optical phonons (OPs) in graphene and graphite measured by time-resolved anti-Stokes Raman scattering. Lifetimes in graphite and monolayer graphene are 2.4 and 1.2 ps, respectively. For graphite and graphene with more than five layers, the lifetimes decrease with increasing temperature as $\sim 1/T$, indicating the dominance of anharmonic processes in the decay of the OP population. The decrease in lifetime with decreasing number of layers suggests an additional decay channel through which excitations in graphene interact directly with lattice vibrations of the a-SiO_2 substrate.

DOI: 10.1103/PhysRevB.81.165405 PACS number(s): 63.20.K−, 63.22.−m

I. INTRODUCTION

In recent years, graphene has been intensely studied as a material for nanoscale electronic devices because of its high mobility and ballistic charge transport on micron length scales.[1–3] The current density in graphene saturates[4,5] at a bias of a few volts; similar behavior has been observed in metallic nanotubes.[6–8] For metallic nanotubes, saturation of the current density at high fields is usually attributed to the onset of optical phonon (OP) emission.[6–9] However, the cause of current saturation in graphene remains controversial. Barreiro *et al.*[4] considered the role of elastic electronic scattering by charged and neutral impurities and argued that hot OPs made a negligible contribution to high-field transport. Meric *et al.*[5] observed current saturation in graphene field-effect transistors and found that the saturation velocity is dependent on the charge-carrier concentration; they attributed this dependence to scattering of electrons and holes in graphene by 55 meV surface phonons in the a-SiO_2 substrate. This remote scattering mechanism by polar substrate phonons has also been invoked in explanations of heat dissipation in nanotube[10] and graphene devices.[11] A better understanding of the decay channels and lifetimes of OP populations will clarify the cause of current saturation and thereby facilitate the design of high-performance graphene electronics.

We employ time-resolved incoherent anti-Stokes Raman scattering (TRIARS) (Refs. 12–15) using a subpicosecond pump-probe method to directly measure the lifetime of zone-center OPs. In TRIARS, a pump optical pulse excites electronic excitations that subsequently generate nonequilibrium OPs; a time-delayed probe optical pulse tracks the generation and decay of nonequilibrium OPs by monitoring the intensity of spontaneous anti-Stokes Raman scattering.[16] Recently, TRIARS was used to measure the lifetime of OPs in carbon nanotubes[13,14] and graphite.[15]

OP lifetimes are often estimated from the Raman linewidth, $\Gamma=(\pi c T_2)^{-1}$, where T_2 is phonon dephasing time. The relaxation time T_1 of the phonon population is equal to half of T_2, $T_1=T_2/2$, only when the rate of pure dephasing is negligible. In semiconducting nanotubes, pure dephasing processes are weak and OP lifetimes estimated from Raman linewidth are comparable to OP lifetimes measured by TRIARS.[13,14] Strong electron-phonon coupling in metallic nanotubes and graphite may lead to substantial dephasing processes and broadening of the Raman linewidth;[17] $T_2/2$ estimated from the Raman linewidth is on the order of ~ 0.1 ps, much shorter than T_1 measured by TRIARS.[13,15]

In this paper, OP lifetimes in both graphene and graphite are measured by TRIARS as a function of substrate temperature and the number of carbon layers. We observe that (a) OP lifetimes of multilayer graphene decrease monotonically with decreasing number of layers; (b) for graphite and >5-layer graphene, OP lifetimes follow a $\sim 1/T$ temperature dependence; and (c) OP lifetimes of monolayer graphene deviates from a $1/T$ temperature dependence. A $1/T$ temperature dependence[18] suggests the dominance of three-phonon anharmonic processes in the decay of the OP population in thick graphene and graphite while a reduction in OP lifetime with decreasing number of layers suggests an additional delay channel such as the coupling of excitations in graphene to substrate phonons.

II. EXPERIMENTAL DETAILS

Graphene samples are prepared by mechanical exfoliation of highly oriented pyrolytic graphite on a-SiO_2/Si substrates with 300-nm-thick oxide layers.[19] For thick graphene layers, the number of layers is determined by contrast observed by optical microscopy;[20] for thin graphene layers, the number of layers is determined by Raman spectroscopy using 633 nm excitation, 1.3 mW laser power, and a spot size of ~ 1 μm. The shape and position of the G band[21–23] and the ratio of the intensity $I_{G'}$ of the G′ band to the intensity I_G of the G band[22–26] are often used to determine the thickness and structure of graphene. The G′ band of our monolayer graphene sample is centered at 2642 cm^{-1}, in agreement with the G′ frequency reported in Refs. 21 and 23. This peak position is easily distinguished from the G′ peak position of misoriented bilayer graphene that appears at 2650 cm^{-1}.[23] In our data, the intensity ratio, $I_{G'}/I_G \approx 4.8$ is not in agreement with Ref. 23. We attribute this discrepancy to small differences in the thickness of the oxide,[27] and possible differences in the wavelength dependence of the quantum efficiency of the charge-coupled device (CCD) camera and the transmission coefficients of the optics. The intensity ratio is still useful,

however, for identifying bilayer graphene since the G band intensity of bilayer graphene is approximately doubled in comparison to monolayer graphene while the G′ band intensity is nearly constant.[22,24,26] Because the Raman spectrum of >5-layer graphene is indistinguishable from that of graphite, we use contrast in optical microscopy images to determine the number of layers; in our two thick graphene samples, the number of layers is 5–6 and 10–12.

To achieve an intrinsic graphene sample—i.e., to avoid adsorption of oxygen and the resulting shifts in the Fermi level away from charge-neutral Dirac point energy, E_o—the samples are annealed in a N_2 environment at 573 K for 2 h and maintained in a N_2 environment[28] during the TRIARS measurement. As a result of this annealing, the position of the G band downshifts by ~4 cm^{-1} and the full width at half maximum (FWHM) of the G band increases by ~8 cm^{-1}, indicating that the Fermi level shifts toward E_o.[28–31] This annealing procedure suppresses the appearance of D band Raman scattering that can be induced by heating under oxygen-rich environments[32] and should also be effective in removing adsorbed water vapor and other volatile contaminants at the graphene/a-SiO_2 interface.

A mode-locked Ti:sapphire laser with an 80 MHz repetition rate[12,33] is used for TRIARS. The pump and probe beams are cross polarized and focused to $1/e^2$ radii of 3.75 μm; the incident pump fluence is 0.40 mJ cm^{-2} and the probe beam fluence is 0.27 mJ cm^{-2}. Raman backscattered light is detected by a thermoelectrically cooled, CCD camera at the output of an imaging spectrograph. Exclusion of depolarized Raman scattering created by the pump beam is achieved by "two-tint" pump-probe method[13,33] based on optical filters and the broad bandwidth of the Ti:sapphire laser oscillator. In our two-tint method for TRIARS, the laser oscillator is tuned to a bandwidth of 10 nm and a central wavelength of 787 nm. To slice the broad bandwidth of the laser oscillator, we place a long-wave pass optical filter with a cutoff of 790 nm in the path of the pump and a narrow band-pass filter with a transmission band of 785 ± 1.5 nm in the path of the probe.

Absorption of the laser beam produces both transient and steady-state heating of the samples. Due to the high thermal conductivity of Si, ≈140 W m^{-1} K^{-1}; the small optical absorption coefficient of Si at this wavelength, ≈1000 cm^{-1}; the low thermal conductivity of a-SiO_2, ≈1.3 W m^{-1} K^{-1}; and the small thickness of graphene, most of the steady-state temperature drop appears across the a-SiO_2 layer. The average steady-state temperature rise is then

$$\Delta T_{dc} = \frac{A(1-R)Ph}{\pi\omega_0^2\Lambda}, \tag{1}$$

where A is the fraction of the laser power that is absorbed in the sample, R is the optical reflectivity, $P=24$ mW is the total laser power in the pump and probe beam, h is the thickness of the SiO_2 layer, ω_0 is the laser beam radius, and Λ is the thermal conductivity of a-SiO_2. For graphite, $A=1$, $R=0.38$, and $\Delta T_{dc} \approx 40$ K. We expect that this steady-state temperature rise in graphite produces a ~10% decrease in the phonon lifetime under the assumption that the temperature dependence of the lifetime scales as $1/T$. For graphene samples, steady-state heating has a negligible effect on the lifetime.

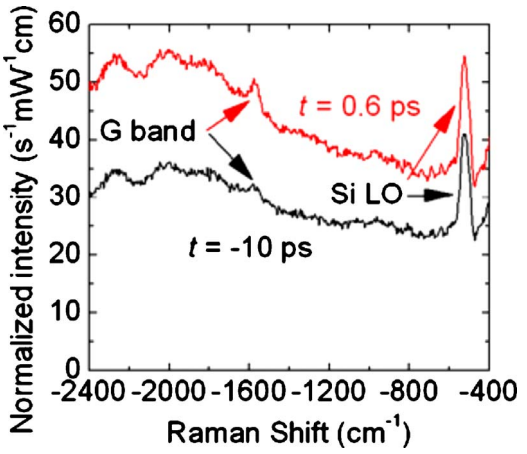

FIG. 1. (Color online) Time-resolved anti-Stokes Raman spectra for monolayer graphene normalized by the integration time, power in the probe beam, and spectral width of one CCD pixel. The lower curve is for a time delay between pump and probe of $t=-10$ ps (black line) and the upper curve is for $t=0.6$ ps (red line). The oscillations in the data at <-1800 cm^{-1} are artifacts from optical interference in the CCD detector.

In addition to the steady-state temperature rise ΔT_{dc}, each optical pulse in the pump beam produces a transient change in the temperature of the sample,

$$\Delta T_p = \frac{A(1-R)F}{Cn}, \tag{2}$$

where C is the heat capacity per unit area of graphene, n is the number of layers, and F is the fluence of the pump beam. Equation (2) is approximately valid for time scales between the phonon relaxation time T_1 and the thermal relaxation time for heat dissipation from graphene into the a-SiO_2 substrate. For n-layer graphene (LG), we calculate R and A using thin film optics;[34] for example, for 1-LG (monolayer graphene), $A=0.009$ and $R=0.3$ and $\Delta T_p=50$ K. For graphite, the optical absorption length corresponds to $n=98$ and $\Delta T_p=49$ K. Since transient heating of monolayer graphene and graphite are similar, we are confident that the observed differences in OP lifetimes between graphene and graphite are not caused by differences in transient heating.

III. RESULTS AND DISCUSSION

Figure 1 shows time-resolved anti-Stokes Raman spectra of monolayer graphene measured by the ultrafast probe pulses after subtraction of depolarized Raman scattering created by the pump pulses.[33] At a time delay between pump and probe pulses of $t=0.6$ ps, the population of OPs is close to its maximum. The intensity of the G band Raman scattering centered at -1580 cm^{-1} is proportional to the population of zone-center OPs. The peaks centered at -520 and -960 cm^{-1} are due to first-order and second-order Raman scattering by phonons in the Si substrate. We have not observed significant D band Raman scattering in any of our

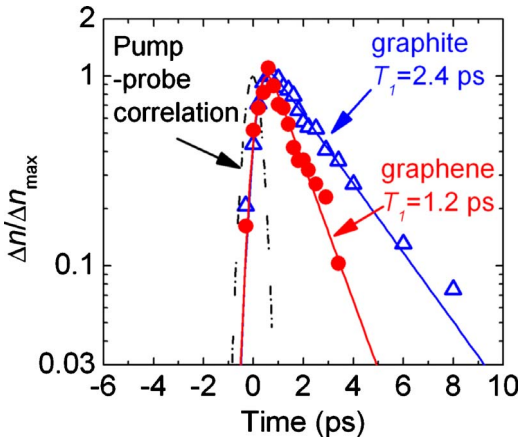

FIG. 2. (Color online) Normalized intensity change of anti-Stokes G band Raman scattering in graphite and monolayer graphene at room temperature as a function of delay time t. Symbols (open blue triangles for graphite, solid red circles for monolayer graphene) and the solid lines are the experimental data and model fits, respectively. The extracted exponential relaxation times for graphite and monolayer graphene from these fits are $T_1=2.4\pm0.1$ ps and $T_1=1.2\pm0.1$ ps, respectively. The time correlation between the pump and probe was measured by two-photon absorption in a GaP photodiode and is shown as a black dashed-dot line; the pump-probe correlation has a FWHM of 0.7 ps.

TRIARS experiments and conclude that graphene is not damaged by the laser fluence we use in our experiments.[35] We attribute the broad peak centered at -2000 cm^{-1} to Raman scattering by nonequilibrium electronic excitations; this electronic scattering is not observable with cw laser excitation.

The intensity of the anti-Stokes G band measured by a cw laser beam is too small to be detected in our apparatus while the intensity excited by a pulsed probe beam alone, i.e., with the pump blocked, is measurable. This implies that even at negative delay times, $t<0$, the population of OPs measured by the probe beam is significantly larger than the equilibrium population because photons near the end of the probe pulse scatter from OPs that have been created since the beginning of the probe pulse.[13]

Temporal evolutions of the integrated intensity of G band Raman scattering measured at room temperature are plotted in Fig. 2; $\Delta n(t)$ is the difference between the OP populations measured at $t=-10$ ps and a pump-probe delay time t. To analyze this data, we model the temporal evolution by an abrupt but time-delayed rise of OP population emitted by hot carriers at a delay time t_0 followed by an exponential decay with a time constant T_1. The data are fit by a convolution of this response function with the cross correlation of the pump and probe. Thus, fits of our model to the data have three free parameters:[12,13] (i) the onset time of OP Raman scattering t_0, (ii) the OP lifetime T_1, and (iii) the amplitude of the change in the signal at $t_0=0^+$. The OP lifetime extracted from these fits for graphite and monolayer graphene at room temperature are 2.4 ± 0.1 ps and 1.2 ± 0.1 ps, respectively. The OP lifetime of graphite is within the experimental uncertainties of the recently reported value of $T_1=2.2\pm0.1$ ps from Ref. 15. The onset times, $t_0=0.15\pm0.1$ ps in both graphene and graphite, are consistent with previous measurements of the initial relaxation times of hot electrons and holes.[36–38]

In graphene under ultrafast pulsed laser irradiation, hot carriers excited by the pump beam rapidly exchange their energy with the Ops (Ref. 38) because of the small heat capacity of the charge carriers and their strong coupling to the Γ-E_{2g} LO and $\mathbf{K}$-A_1' modes.[39,40] This exchange of energy between hot carriers and OP occurs on a time scale of ≈150 fs. On time scales >150 fs, the carriers and OPs are essentially in equilibrium and the relaxation of hot carriers[39,41] is controlled by the relatively slow exchange of energy between the OPs and the other vibrational modes of the lattice.

A slow relaxation of hot carriers has been observed previously by ultrafast optical pump-probe spectroscopy.[36,42,43] Wang *et al.*[42] used the slow relaxation time measured in transient absorption measurements to determine the OP lifetimes by fitting the data to coupled rate equations. The OP lifetime derived in this way ≈2.5 ps was independent of the number of layers, type of substrate, and Raman intensity ratio, I_G/I_D. However, the time constant of the slow relaxation observed in Ref. 42 does not agree with the results of two prior pump-probe studies, see Refs. 36 and 43. The authors of Ref. 43, reported that the time constant increases from 2.5 to 5 ps as the number of layer increases from 1 to ~30 and saturates at 5 ps for >30 layer graphene; they attributed this thickness dependence to coupling to the substrate. In addition to the intended sensitivity to optical phonon lifetime,[42] transient absorption data may also have unintended sensitivity to contributions from carrier recombination and relaxation via acoustic phonons.[43] The time constants of the slow relaxation observed in Ref. 36 are in the range of 0.4–1.7 ps and proportional to Raman intensity ratio, I_G/I_D.

In contrast to the transient absorption experiments discussed above, TRIARS provides a direct measurement of the population lifetime of near-zone-center optical phonons. Our measurements of the thickness and temperature dependence of OP lifetimes in graphene and graphite are summarized in Fig. 3. Lifetimes of multilayer graphene increase monotonically with increasing number of layers. For >5-layer graphene and for graphite, the OP lifetimes decrease with increasing temperature T with a dependence that is consistent with $1/T$. This observation suggests that the population lifetime is mostly controlled by a three-phonon anharmonic process, e.g., the decay of one OP into two acoustic phonons.[18] On the other hand, the OP lifetimes in monolayer graphene are less dependent on temperature and deviate from the $1/T$ dependence expected for three-phonon decay.

The intrinsic Raman linewidths Γ^{in} of G band in graphene and graphite are often assumed to be a sum of the electron-phonon (e-ph) interactions $\Gamma^{e\text{-}p}$ and anharmonic phonon-phonon (p-p) interactions $\Gamma^{p\text{-}p}$; $\Gamma^{in}=\Gamma^{e\text{-}ph}+\Gamma^{p\text{-}p}$.[28,44] The calculated $\Gamma^{p\text{-}p}$ of both graphene and graphite of ≈2 cm^{-1},[44] which translates into $T_2/2\approx T_1\approx2.65$ ps, is comparable to our measured OP lifetime of $T_1=2.4\pm0.1$ ps in graphite. The good agreement between the calculated phonon lifetime based on anharmonic interactions and our observation of a $1/T$ temperature dependence supports the conclusion that anharmonic processes are the main decay channel in TRIARS measurements of OPs in graphite and thick graphene.

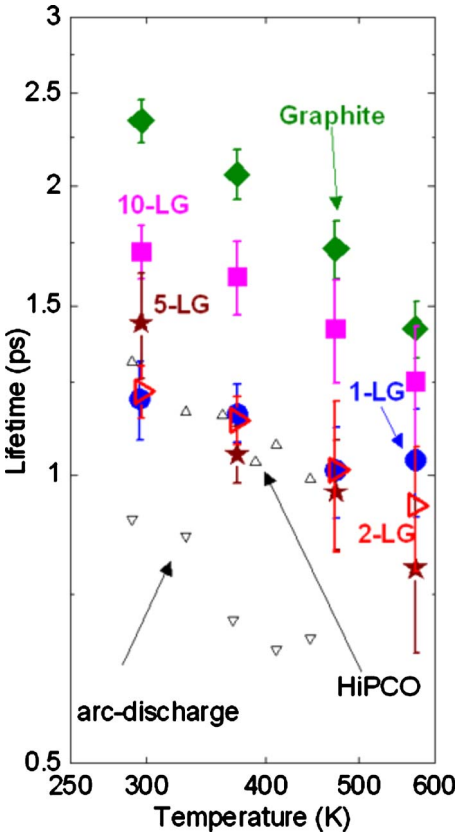

FIG. 3. (Color online) Lifetimes of OPs in graphite (solid green diamonds), thick-layer graphene (solid pink squares), 5-LG (solid brown stars), bilayer graphene (open red triangles), and monolayer graphene (solid blue circles) as a function of the temperature of the substrate. Data for the lifetime of the OP in HiPCO nanotubes (open black triangles) and arc-discharge nanotubes (open black inverted triangles) from Ref. 13 are included for comparison. Error bars are assigned from the uncertainties in the model fits.

Because of the weak interaction between graphite planes, we could expect that the OP lifetime in graphene would be comparable to the lifetime in graphite.[45] However, our measured OP lifetime of $T_1 = 1.2 \pm 0.1$ ps in monolayer graphene is 50% of the lifetime of graphite. This result implies that OPs in monolayer graphene decay by a channel other than the three-phonon anharmonic process and the strength of this additional channel is comparable to the anharmonic decay channel in graphite.

Although we cannot conclusively determine the origin of this additional decay channel in graphene through our experiments alone, we consider possible effects of the a-SiO_2 substrate. The scattering of charge carriers in nanotubes and graphene by optical phonons in a-SiO_2 is often considered to be a critical factor in devices built on a-SiO_2 substrates.[5,46–48] The strength of electrostatic interaction between charge carriers in graphene and the polar modes of the SiO_2 substrate is strong, two orders of magnitude higher than the interaction with charged impurities.[49] We speculate that the shorter OP lifetimes we observe in our graphene experiments are caused by an additional decay channel where OPs in graphene exchange energy with charge carriers which, in turn, transfer energy to polar phonons of the substrate.

To estimate how fast energy could be exchanged across the interface through this mechanism, we estimate the thermal time constant of the coupled electron/OP system as $\tau = C_{OP}/G$, where C_{OP} is the heat capacity per unit area of hot OPs in monolayer graphene and G is the effective value of the interfacial thermal conductance for energy transport between the hot carriers and the substrate phonons. As an order-of-magnitude estimate for C_{OP}, we assume that the heat capacity of the highly excited OPs follows the classical Dulong-Petit law, and that 3% of all OP modes are excited[15] by the pump beam: $C_{OP} \approx 2.2 \times 10^{-5}$ J m^{-2} K^{-1}. In Ref. 11, the interfacial thermal conductance between hot carriers and an a-SiO_2 substrate was estimated as $G \approx 24$ MW m^{-2} K^{-1}. From these values of C_{OP} and G, we find $\tau \sim 1$ ps. This calculation has large uncertainties but the correct order of magnitude of the result supports the idea that remote scattering of charge carriers by polar phonons in a-SiO_2 could be playing a role in the faster decay of OPs in monolayer graphene.

We can also estimate the OP lifetimes in multilayer graphenes with the same approach in combination with the assumption that the effect of remote scattering by substrate phonons scales with distance z as $\sim 1/z^2$.[49] Since anharmonic process and remote scattering by polar phonons should act in parallel, we write the thermal time constants as $\tau = nC_{OP}/(G_n + nD)$ where n is the number of layers, and D is the intrinsic effective thermal conductance that couples OP to other vibrational modes by anharmonic process. We use the OP lifetime of graphite to estimate D and find $D \approx 9$ MW m^{-2} K^{-1}. G_n is total conductance that couples the electronic excitations in n-LG to the polar phonons of the a-SiO_2 substrate. For 5-LG and 10-LG, this calculation predicts $\tau \sim 1.5$ ps and $\tau \sim 1.9$ ps, respectively. The thickness of 10-LG is much smaller than the optical penetration depth of graphite at 785 nm and, therefore, the measured Raman spectrum in 10-LG originates from the entire thickness of the sample.

Of course, TRIARS measurements of graphene that is suspended over an opening or trench would be an important follow up to the experiments we describe here. We have not yet been able to apply TRIARS to suspended n-LG graphene because of a variety of experimental challenges, mostly related to the need for a relatively large area of suspended sample with a homogenous thickness. (The apparatus we use to anneal the samples and maintain a N_2 environment requires a relatively large working distance that limits the laser spot size to ≈ 8 μm diameter.) Nevertheless, we believe that such measurements should be possible as long as the additional steady-state temperature rise of the sample can be understood and controlled.

Finally, we discuss the possible effects of "ripple" vibrational modes on the OP lifetime. Because bilayer graphene is more rigid and therefore shows significantly weaker ripple modes than monolayer graphene,[3] the effect of ripples modes on energy transport in graphene is dominant only in monolayer graphene. However, the difference between the OP lifetimes of monolayer graphene and bilayer graphene is small, see Fig. 3, and we conclude that ripple modes do not have a strong effect on the decay of OPs in graphene.

In conclusion, we present experimental data for the OP lifetime in graphite and graphene as a function of tempera-

ture and thickness. Anharmonic processes are dominant for OP decay in graphite and thick graphene. Coupling between charge carriers in graphene and polar phonons in the a-SiO_2 substrate may provide an additional decay channel in thin and monolayer graphene.

ACKNOWLEDGMENTS

This material is based upon work supported by the U.S. Department of Energy, Division of Materials Sciences under Grant No. DE-FG02-07ER46459, through the Frederick Seitz Materials Research Laboratory at the University of Illinois at Urbana-Champaign. Experiments were carried out in part in the Frederick Seitz Materials Research Laboratory Central Facilities, University of Illinois, which are partially supported by the U.S. Department of Energy under Grants No. DE-FG02-07ER46453 and No. DE-FG02-07ER46471. This material is also based in part upon work supported by the National Science Foundation under Grant No. DMR-0905175.

*Corresponding author. Present address: School of Mechanical Engineering, Yonsei University, Seoul 120-749, Korea. kgkang09@gmail.com

[1] K. I. Bolotin, K. J. Sikes, J. Hone, H. L. Stormer, and P. Kim, Phys. Rev. Lett. **101**, 096802 (2008).
[2] X. Du, I. Skachko, A. Barker, and E. Y. Andrei, Nat. Nanotechnol. **3**, 491 (2008).
[3] S. V. Morozov, K. S. Novoselov, M. I. Katsnelson, F. Schedin, D. C. Elias, J. A. Jaszczak, and A. K. Geim, Phys. Rev. Lett. **100**, 016602 (2008).
[4] A. Barreiro, M. Lazzeri, J. Moser, F. Mauri, and A. Bachtold, Phys. Rev. Lett. **103**, 076601 (2009).
[5] I. Meric, M. Y. Han, A. F. Young, B. Ozyilmaz, P. Kim, and K. L. Shepard, Nat. Nanotechnol. **3**, 654 (2008).
[6] Z. Yao, C. L. Kane, and C. Dekker, Phys. Rev. Lett. **84**, 2941 (2000).
[7] A. Javey, J. Guo, M. Paulsson, Q. Wang, D. Mann, M. Lundstrom, and H. Dai, Phys. Rev. Lett. **92**, 106804 (2004).
[8] E. Pop, D. Mann, J. Cao, Q. Wang, K. Goodson, and H. Dai, Phys. Rev. Lett. **95**, 155505 (2005).
[9] M. Lazzeri, S. Piscanec, F. Mauri, A. C. Ferrari, and J. Robertson, Phys. Rev. Lett. **95**, 236802 (2005).
[10] S. V. Rotkin, V. Perebeinos, A. G. Petrov, and P. Avouris, Nano Lett. **9**, 1850 (2009).
[11] M. Freitag, M. Steiner, Y. Martin, V. Perebeinos, Z. Chen, J. C. Tsang, and P. Avouris, Nano Lett. **9**, 1883 (2009).
[12] J. J. Letcher, K. Kang, D. G. Cahill, and D. D. Dlott, Appl. Phys. Lett. **90**, 252104 (2007).
[13] K. Kang, T. Ozel, D. G. Cahill, and M. Shim, Nano Lett. **8**, 4642 (2008).
[14] D. Song, F. Wang, G. Dukovic, M. Zheng, E. D. Semke, L. E. Brus, and T. F. Heinz, Phys. Rev. Lett. **100**, 225503 (2008).
[15] H. Yan, D. Song, K. F. Mak, I. Chatzakis, J. Maultzsch, and T. F. Heinz, Phys. Rev. B **80**, 121403(R) (2009).
[16] A. Laubereau and W. Kaiser, Rev. Mod. Phys. **50**, 607 (1978).
[17] M. Lazzeri, S. Piscanec, F. Mauri, A. C. Ferrari, and J. Robertson, Phys. Rev. B **73**, 155426 (2006).
[18] P. G. Klemens, Phys. Rev. **148**, 845 (1966).
[19] Y. B. Zhang, Y. W. Tan, H. L. Stormer, and P. Kim, Nature (London) **438**, 201 (2005).
[20] P. Blake, E. W. Hill, A. H. Castro Neto, K. S. Novoselov, D. Jiang, R. Yang, T. J. Booth, and A. K. Geim, Appl. Phys. Lett. **91**, 063124 (2007).
[21] A. C. Ferrari, J. C. Meyer, V. Scardaci, C. Casiraghi, M. Lazzeri, F. Mauri, S. Piscanec, D. Jiang, K. S. Novoselov, S. Roth, and A. K. Geim, Phys. Rev. Lett. **97**, 187401 (2006).
[22] Z. H. Ni, Y. Y. Wang, T. Yu, Y. M. You, and Z. X. Shen, Phys. Rev. B **77**, 235403 (2008).
[23] P. Poncharal, A. Ayari, T. Michel, and J. L. Sauvajol, Phys. Rev. B **78**, 113407 (2008).
[24] Y. Y. Wang, Z. H. Ni, Z. X. Shen, H. M. Wang, and Y. H. Wu, Appl. Phys. Lett. **92**, 043121 (2008).
[25] D. M. Basko, S. Piscanec, and A. C. Ferrari, Phys. Rev. B **80**, 165413 (2009).
[26] D. Graf, F. Molitor, K. Ensslin, C. Stampfer, A. Jungen, C. Hierold, and L. Wirtz, Nano Lett. **7**, 238 (2007).
[27] D. Yoon, H. Moon, Y.-W. Son, J. S. Choi, B. H. Park, Y. H. Cha, Y. D. Kim, and H. Cheong, Phys. Rev. B **80**, 125422 (2009).
[28] D. Abdula, T. Ozel, K. Kang, D. G. Cahill, and M. Shim, J. Phys. Chem. C **112**, 20131 (2008).
[29] J. Yan, Y. B. Zhang, P. Kim, and A. Pinczuk, Phys. Rev. Lett. **98**, 166802 (2007).
[30] A. Das, S. Pisana, B. Chakraborty, S. Piscanec, S. K. Saha, U. V. Waghmare, K. S. Novoselov, H. R. Krishnamurthy, A. K. Geim, A. C. Ferrari, and A. K. Sood, Nat. Nanotechnol. **3**, 210 (2008).
[31] S. Berciaud, S. Ryu, L. E. Brus, and T. F. Heinz, Nano Lett. **9**, 346 (2009).
[32] L. Liu, S. Ryu, M. R. Tomasik, E. Stolyarova, N. Jung, M. S. Hybertsen, M. L. Steigerwald, L. E. Brus, and G. W. Flynn, Nano Lett. **8**, 1965 (2008).
[33] K. Kang, Y. K. Koh, C. Chiritescu, X. Zheng, and D. G. Cahill, Rev. Sci. Instrum. **79**, 114901 (2008).
[34] K. Kang, S. H. Lee, H. S. Ryou, Y. K. Choi, S. Park, and J. S. Lee, Mater. Trans. **49**, 1880 (2008).
[35] B. Krauss, T. Lohmann, D.-H. Chae, M. Haluska, K. von Klitzing, and J. H. Smet, Phys. Rev. B **79**, 165428 (2009).
[36] J. M. Dawlaty, S. Shivaraman, M. Chandrashekhar, F. Rana, and M. G. Spencer, Appl. Phys. Lett. **92**, 042116 (2008).
[37] K. Ishioka, M. Hase, M. Kitajima, L. Wirtz, A. Rubio, and H. Petek, Phys. Rev. B **77**, 121402(R) (2008).
[38] P. A. George, J. Strait, J. Dawlaty, S. Shivaraman, M. Chandrashekhar, F. Rana, and M. G. Spencer, Nano Lett. **8**, 4248 (2008).
[39] S. Butscher, F. Milde, M. Hirtschulz, E. Malic, and A. Knorr, Appl. Phys. Lett. **91**, 203103 (2007).
[40] S. Piscanec, M. Lazzeri, F. Mauri, A. C. Ferrari, and J. Robertson, Phys. Rev. Lett. **93**, 185503 (2004).
[41] M. Richter, A. Carmele, S. Butscher, N. Bücking, F. Milde, P. Kratzer, M. Scheffler,and A. Knorr, J. Appl. Phys. **105**, 122409 (2009).

[42] H. Wang, J. H. Strait, P. A. George, S. Shivaraman, V. B. Shields, M. Chandrashekhar, J. Hwang, F. Rana, M. G. Spencer, C. S. Ruiz-Vargas, and J. Park, Appl. Phys. Lett. **96**, 081917 (2010).
[43] R. W. Newson, J. Dean, B. Schmidt, and H. M. van Driel, Opt. Express **17**, 2326 (2009).
[44] N. Bonini, M. Lazzeri, N. Marzari, and F. Mauri, Phys. Rev. Lett. **99**, 176802 (2007).
[45] N. Bonini, R. Rao, A. M. Rao, N. Marzari, and J. Menendez, Phys. Status Solidi B **245**, 2149 (2008).
[46] S. Fratini and F. Guinea, Phys. Rev. B **77**, 195415 (2008).
[47] M. Steiner, M. Freitag, V. Perebeinos, J. C. Tsang, J. P. Small, M. Kinoshita, D. Yuan, J. Liu, and P. Avouris, Nat. Nanotechnol. **4**, 320 (2009).
[48] A. G. Petrov and S. V. Rotkin, JETP Lett. **84**, 156 (2006).
[49] J. Sabio, C. Seoánez, S. Fratini, F. Guinea, A. H. Castro Neto, and F. Sols, Phys. Rev. B **77**, 195409 (2008).